Journal of Mathematics and Informatics
Vol. 1, 2013-14, 34-42
ISSN: 2349-0632 (P), 2349-0640 (online)
Published on 1 October 2013
www.researchmathsci.org

Journal of
Mathematics and Informatics

Augmented Lagrangian method for image restoration with spatially adapted parameter selection

***Jin-Hua Chen*[1], *Xiang-Lian Yu*[1], *Xiao-Guang Lv*[1], *Shun-Xu* Wang[1], *Le Jiang*[1,2]**

[1]School of Science, Huaihai Institute of Technology
Lianyungang, Jiangsu, 222005, P.R. China
E-mail: xiaoguanglv@126.com

[2]School of Mathematical Sciences,
University of Electronic Science and Technology of China
Chengdu, Sichuan, 611731, P.R. China

Received 01 July 2013; accepted 16 July 2013

Abstract. The aim of image restoration is to reconstruct an approximation of an image from blurred and noisy measurements. The problem has received considerable attention in recent years. In this paper, we propose the augmented Lagrangian method to restore blurred and noisy images with spatially adapted regularization parameter selection. Some numerical examples are given to illustrate the effectiveness of the proposed algorithm.

Keywords: Image restoration; Augmented Lagrangian method; Parameter selection; Total variation; Regularization

AMS Mathematics Subject Classification (2010): 65Yxx, 68Wxx

1. Introduction

The recording of an image usually involves a degradation process: a blurrring, due to atmosphere turbulence, camera misfocus or relative movement, followed by a random noise, due to errors of the physical sensors or to quantization [1,2,3]. The goal of image restoration is to reconstruct an approximation of an image from a blurred and noisy measurement. Image restoration plays an important part in various areas of applied sciences such as medical imaging, microscopy, astronomy, film restoration, and image and video coding [4, 5, 6]. The image formation process is typically modeled as

$$g = Hf + e, \tag{1}$$

where $f \in R^{n^2}$ represents the ideal $n \times n$ image, $g \in R^{n^2}$ represents the observed $n \times n$ image, $e \in R^{n^2}$ represents the additive noise and the structured matrix $H \in R^{n^2 \times n^2}$ related to the boundary conditions is called a blurring matrix that models the blurring operation. In this work, we assume that the norm of the noise $\sigma = \|e\|_2$ is explicitly known, but that the noise vector e is not.

Mathematically, image restoration is a typical ill-posed inverse problem. It is known that the solution of $Hf = g$ is very sensitive to the noise e in the right-hand side g. To stabilize the recovery of the image f, one must utilize some prior information. In such a stabilization scheme, a common approach is to add a regularizer to the data fidelity term, resulting to the following reconstruction model:

$$\min_f \frac{1}{2}\|Hf - g\|_2^2 + \lambda \mathrm{Reg}(f), \qquad (2)$$

where in the objective function, $\mathrm{Reg}(f)$ regularizes the solution by enforcing certain prior constraints and λ is the regularization parameter that controls the balance between the fidelity term and the regularization term for minimization.

Probably one of the most popular regularization methods is Tikhonov regularization [7]. The regularization functionals used more often are quadratic functionals of the form $\mathrm{Reg}(f) = \|Lf\|_2^2$, where L is usually chosen to be the identity matrix or differentiation matrix. This choice essentially gives a linear least squares problem, but has the drawback of penalizing discontinuities in the image f. Therefore, this is not a good choice if we are interested in edge restoration. To overcome this shortcoming, Rudin, Osher and Fatemi [8] proposed a total variation (TV)-based regularization technique (ROF model), which preserves the edge information in the restored image. In this case, the regularization term is the TV-norm: $\mathrm{Reg}(f) = \|\nabla f\|_1$. To define the discrete TV-norm, we usually introduce the discrete gradient ∇f as follows [9]:

$$(\nabla f)_{i,j} = \left((\nabla f)_{i,j}^x, (\nabla f)_{i,j}^y\right)$$

with

$$(\nabla f)_{i,j}^x = \begin{cases} f_{i+1,j} - f_{i,j}, & i < n, \\ 0, & i = n \end{cases} \text{ and } (\nabla f)_{i,j}^y = \begin{cases} f_{i,j+1} - f_{i,j}, & j < n, \\ 0, & j = n. \end{cases}$$

Here $f_{i,j}$ represents the value of pixel (i,j) in the image, it is the $(i + (n-1)j)$ th entry of the vector image f. With the notations, the discrete TV-norm of f is defined as follows:

$$\|\nabla f\|_1 = \sum_{i,j=1}^{n} \left|(\nabla f)_{i,j}\right| = \sum_{i,j=1}^{n} \sqrt{\left((\nabla f)_{i,j}^x\right)^2 + \left((\nabla f)_{i,j}^y\right)^2}, \qquad (3)$$

where $|y| = \sqrt{y_1^2 + y_2^2}$ for every $y = (y_1, y_2) \in R^2$. In fact, as reported in [10], we can use the periodic boundary condition for the discrete TV-norm. It is well known that the major difficulty of the ROF model is the high nonlinearity and non-differentiability of the object function. To address the problem, many efficient and robust methods have been proposed; see [11,12,13,14,15] for more details.

Clearly, the choice of the regularization parameter λ in (2) is a non-trivial issue. A large λ favors a small solution norm at the cost of a large residual norm, while a small

λ has the opposite effect. Thus, the regularization λ is an important quantity which controls the properties of the regularized solution, and λ should therefore be chosen with care. Throughout the years a variety of parameter choice strategies such as the discrepancy principle, the L-curve and generalized cross validation (GCV) have been developed [16,17]. In particular, total variation models with a spatially varying choice of parameters were considered in [18,19,20,21]. Motivated by these works, Dong, Hintermuller and Rincon-Camacho [22] introduced a robust multi-scale total variation model for image restoration recently. The model utilizes a spatially dependent regularization parameter in order to enhance image regions containing details while still sufficiently smoothing homogeneous features. The fully automated adjustment strategy of the regularization parameter is based on local variance estimators.

In this paper, we consider to deal with the automated regularization parameter selection model proposed in [22] by the augmented Lagrangian method. The proposed algorithm is much faster than the primal-dual approach of [22] for the spatially adapted total variation model. Our numerical results show that our method outperforms some existing restoration methods in terms of the Peak-Signal-to-Noise Ratio (PSNR) and Structural SIMilarity (SSIM) value. The organization of this paper is outlined as follows. In the next section, we recall some basic results of the augmented Lagrangian method for image restoration. In Section 3, we introduce the automated regularization parameter selection method and propose the augmented Lagrangian method for the solution of the model. Some numerical experiments are given to illustrate the performance of the proposed algorithm in Section 4.

2. Augmented Lagrangian method

Consider an unconstrained optimization problem:

$$\min_u \Psi(u) + \Phi(Du)\,, \tag{4}$$

where Ψ and Φ are proper, closed and convex functions. Introducing a new variable $v = Du$, we can rewrite (4) as a constrained problem of the form:

$$\begin{aligned} &\min_{u,v} \Psi(u) + \Phi(v), \\ &\quad \text{s.t.} Du = v. \end{aligned} \tag{5}$$

The associated augmented Lagrangian function for this problem is defined as

$$L(u,v,b,\eta) = \Psi(u) + \Phi(v) + \frac{\eta}{2}\|Du - v + b\|_2^2, \tag{6}$$

where η is related to the penalty parameter for the constraint in (5). The idea of the augmented Lagrangian method is to find a saddle point of (6), which is also the solution of the original problem (4). We can use the alternating direction method to iteratively solve the following subproblems:

$$\begin{cases} u^{k+1} = \arg\min\limits_{u} \Psi(u) + \dfrac{\eta}{2}\left\|Du - v^k + b^k\right\|_2^2, \\ v^{k+1} = \arg\min\limits_{v} \Phi(u) + \dfrac{\eta}{2}\left\|Du^{k+1} - v + b^k\right\|_2^2, \\ \qquad b^{k+1} = b^k - (Du^{k+1} - v^{k+1}). \end{cases}$$

We now investigate these subproblems one by one for the spatially adapted total variation image restoration problem (2) with a spatially varying parameter. In this case, we have $\Psi(f) = \frac{1}{2}\left\|Hf - g\right\|_2^2$, $\Phi(Df) = \sum_i^{n^2} \lambda_i \left\|D_i f\right\|_2$ where D_i denotes the discrete gradient of f at pixel i.

For the first subproblem, it is required to solve the following normal equation:

$$(H^T H + \eta D^T D) f = H^T g + \eta D^T (v^k + b^k). \tag{8}$$

Under the periodic boundary condition, D and H have block circulant with circulant blocks (BCCB) structure; see [10] for more details. We know that the computations with BCCB matrices can be done very efficiently by using fast Fourier transforms (FFTs). For the second subproblem, we need to solve the following problem:

$$\min_v \sum_{i=1}^{n^2} \lambda_i v_i + \frac{\eta}{2}\left\|Df^{k+1} - v + b^k\right\|_2^2, \tag{9}$$

where $v = (v_1, v_2, ..., v_{n^2})$. It is known that the problem can be solved using a shrinkage formula. We refer to [14] for details. Now we are in a position to describe the augmented Lagrangian method for the total variation image restoration problem with a spatially varying parameter as follows:

Algorithm 1. Augmented Lagrangian method for the total variation image restoration problem with a spatially varying parameter.

Input: v^0, b^0, g and $k = 0$.

1. For v^k and b^k fixed, employ an efficient method to compute f^{k+1}:

$$(H^T H + \eta D^T D) f = H^T g + \eta D^T (v^k + b^k).$$

2. For f^{k+1} and b^k fixed, use a shrinkage formula to compute

$$v^{k+1} = \arg\min_v \sum_{i=1}^{n^2} \lambda_i v_i + \frac{\eta}{2}\left\|Df^{k+1} - v + b^k\right\|_2^2.$$

3. Update $b^{k+1} = b^k - (Du^{k+1} - v^{k+1})$.

4. Check the stopping criteria. If a stopping criterion is satisfied, then exit with an approximate solution; otherwise, let $k = k + 1$ and go to step 1.

3. Spatially adaptive algorithm

In this section, we propose the augmented Lagrangian method for image restoration with spatially adapted parameter selection. At first, we describe how to choose the spatially adapted regularization parameter. For the sake of simplicity, we use the continuous model. Similar to [22], we define a normalized filter:

$$\omega(x,y)=\begin{cases}\dfrac{1}{\left|\Omega_x^r\right|}, & \left\|y-x\right\|_\infty \le \dfrac{r}{2},\\ 0, & \text{othervise}\end{cases}$$

where $x\in\Omega$ is fixed, Ω_x^r is a local window centered at pixel x which is defined by $\Omega_x^r=\left\{y:\left\|y-x\right\|_\infty\le\frac{r}{2}\right\}$ and $r>0$ sufficiently small is the essential width of the filter window. By $F(u)(x)$ we denote the local expected value estimator, which is

$$F(u)(x)=\int_\Omega \omega(x,y)(Hf-g)^2(y)dy\,. \tag{10}$$

Hence, we obtain the following total variation-based minimization problem with local constraints based on formula (10):

$$\min_{u\in s(\Omega)}\int_\Omega\left|\nabla f\right|dx \text{ s.t. } F(u)\le 1+\varepsilon \text{ a.e. in } \Omega \tag{11}$$

where “a.e.” stands for “almost everywhere”. The proof of the existence of a solution in (11) can be found in [22].

In the discrete form, we let $\Omega_{i,j}^r$ denote the set of pixel-coordinates in a r-by-r window centered at (i,j) with a symmetric extension at the boundary, which is

$$\Omega_{i,j}^r=\left\{(s+i,t+j):-\frac{r-1}{2}\le s,t\le\frac{r-1}{2}\right\}.$$

We apply the mean filter to the residual $g-Hf$ and obtain the local expected value estimator:

$$S_{i,j}^r=\frac{1}{r^2}\sum_{(s,y)\in\Omega_{i,j}^r}(g_{s,t}-(Hf)_{s,t})^2\,.$$

Similar to the work in [22], we can propose the similar update scheme of λ as follows:

$$\frac{1}{\tilde{\lambda}_{i,j}^{k+1}}=\frac{1}{\tilde{\lambda}_{i,j}^{k}}+\delta\max((S_k)_{i,j}^r-\sigma^2,0)\,, \tag{12}$$

$$\frac{1}{\lambda_{i,j}^{k+1}}=\frac{1}{r^2}+\sum_{(s,y)\in\Omega_{i,j}^r}\frac{1}{\tilde{\lambda}_{s,t}^{k+1}}\,, \tag{13}$$

where δ is a step size. For obtaining a better choice of the regularization parameter, we can apply a modified local variance estimator $\tilde{S}_{i,j}^r$ to replace $S_{i,j}^r$; see [22] for more details.

Based on the Hierarchical decomposition technique, we have the following augmented Lagrangian method for image restoration with spatially adapted parameter selection.

Algorithm 2. Augmented Lagrangian method for image restoration with spatially adapted parameter selection.

Input: f^0, λ^0 and $k = 0$.

1. If $k = 0$, employ Algorithm 1 with $\lambda = \lambda^0$ to compute:

$$\hat{f}^0 = \arg\min_f \frac{1}{2}\|Hf - g\|_2^2 + \sum_i^{n^2} \lambda_i \|D_i f\|_2,$$

else compute $\hat{f}^k$ by Algorithm 1 with $\lambda = \lambda^k$ and $v^k = g - Hf^k$:

$$\hat{f}^k = \arg\min_f \frac{1}{2}\|Hf - v^k\|_2^2 + \sum_i^{n^2} \lambda_i^k \|D_i f\|_2.$$

2. Update $f^{k+1} = f^k + \hat{f}^k$.

3. Update λ^k based on (12) and (13).

4. Check the stopping criteria. If a stopping criterion is satisfied, then exit; otherwise, let $k = k+1$ and go to step 1.

4. Numerical experiments

In this section, we present numerical results to illustrate the performance of the proposed approach for image restoration. We compare the proposed algorithm (Algorithm 2) with the SATV algorithm presented in [22]. All computations of the present paper were carried out in Matlab 7.10 on a PC with an Intel(R) Core(TM) i3-2130 CPU 3.4 GHz and 4 GB of RAM. The initial guess is chosen to be the black image (zero matrix) in all tests. As reported in [22], we concentrate on image denoising in this work, i.e., H is the identity matrix and use the window size $r = 11$. In this way, we have a fair comparison for our algorithm with the SATV algorithm.

The quality of the restoration results by different methods is compared quantitatively by using the Peak-Signal-to-Noise Ratio (PSNR) and Structural SIMilarity index (SSIM). In general, a high PSNR-value indicates that the restoration is more accurate. The SSIM is a well known quality metric used to measure the similarity between two images. This method is developed by Wang et al. [23], and is based on three specific statistical measures that are much closer to how the human eye perceives differences between images.

Suppose f and $\tilde{f}$ are the original image and the restored image, respectively. The PSNR and SSIM are defined as follows:

$$\text{PSNR} = 20\log_{10}\frac{255n}{\|\tilde{f} - f\|_2}, \tag{14}$$

$$\text{SSIM} = \frac{(2\mu_f\mu_{\tilde{f}} + C_1)(2\sigma_{\tilde{f}f} + C_2)}{(\mu_f^2 + \mu_{\tilde{f}}^2 + C_1)(\mu_f^2 + \mu_{\tilde{f}}^2 + C_2)}, \tag{15}$$

where μ_f and $\mu_{\tilde{f}}$ are averages of f and $\tilde{f}$, respectively. σ_f and $\sigma_{\tilde{f}}$ are the variance of f and $\tilde{f}$, respectively. $\sigma_{\tilde{f}f}$ is the covariance of f and $\tilde{f}$. The positive constants C_1 and C_2 can be thought of as stabilizing constants for near-zero denominator values. We refer the reader to [23] for further details on SSIM.

In the first test, we consider the well-known Cameraman image with size of 256×256. The original image is contaminated by the 2% Gaussian noise. The ideal image and the degraded image are shown in Figures 1(a) and 1(b). The restored images by SATV and the proposed method are shown in Figures 1(c) and 2(d). In this test, we choose the penalty parameter $\eta = 5$ for the proposed method. From the figures, compared with SATV, the proposed method yields better results in image restoration. We observe that the CPU time of the proposed method is much less than that of SATV. We show the SSIM maps and the plots of λ in Figures 1(e)-(h). We see from Figures 1(e) and 1(f) that the SSIM map of the restored image by the proposed algorithm is whiter than that by the SATV algorithm, i.e., our method can get better restoration results.

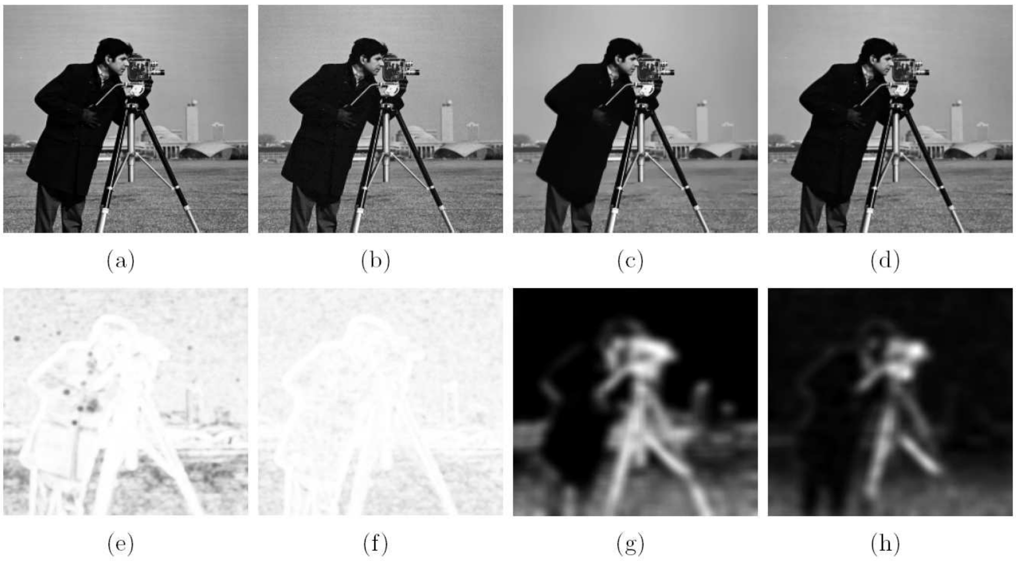

Figure 1. Results of the Cameraman image. (a) Original image. (b) Degraded image. (c) Restored image by SATV (CPU time: 53.70s, PSNR=35.07dB). (d) Restored image by the proposed method (CPU time: 7.76s, PSNR=36.45dB). (e) SSIM map by SATV (SSIM=0.93). (f) SSIM map by the proposed method (SSIM=0.96). (g) Final value of λ in SATV. (h) Final value of λ the proposed method.

In the second example, the 256×256 Lena image shown in Figure 2(a) is degraded by the Gaussian white noise with 5% to generate the observed image displayed in Figure 2(b). The restored images by SATV and the proposed method with $\eta = 10$ are shown Figure 2(c) and 2(d), respectively. It is not difficult to observe that the restored image by our method contains more details. From Figure 2(e) and 2(f), we know that the SSIM value of the restored image by the proposed method is higher than the SATV method. The results in terms of the SSIM map, CPU time and final value of regularization parameter λ show that the performance of the proposed method is superior to that of the SATV method.

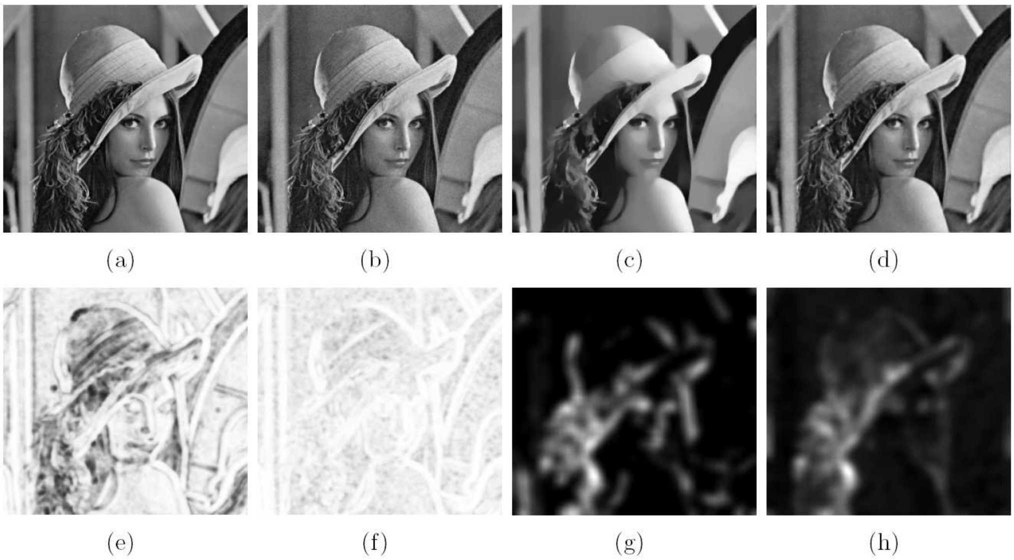

Figure 2. Results of the Lena image. (a) Original image. (b) Degraded image. (c) Restored image by SATV (CPU time: 54.40s, PSNR=28.21dB). (d) Restored image by the proposed method (CPU time: 8.53s, PSNR=31.33dB). (e) SSIM map by SATV (SSIM=0.84). (f) SSIM map by the proposed method (SSIM=0.92). (g) Final value of λ in SATV. (h) Final value of λ the proposed method.

Acknowledgements

This work is supported by the National Training Programs of Innovation and Entrepreneurship for Undergraduates (201211641018), National Natural Science Foundation of China (10871034) and Sichuan Province Sci. & Tech. Research Project (12ZC1802), Jiangsu Province Research Project (12KJD110001).

REFERENCES

1. P. C. Hansen, J. G. Nagy and D. P. O'Leary, Deblurring Images: Matrices, Spectra, and Filtering, SIAM, Philadelphia, 2006.
2. T. F. Chan and J. H. Shen, Image Processing and Analysis: variational, PDE, wavelet, and Stochastic Methods, SIAM, Philadelphia, 2005.
3. T. F. Chan and P. Mulet, Iterative Methods for Total Variation Image Restoration, Technical report, UCLA, 96(38), 1996.
4. H.Andrew and B.Hunt, Digital Image Restoration, Prentice-Hall, Englewood Cliffs, NJ, 1977.

5. M. Banham and A. Katsaggelos, Digital image restoration, IEEE Signal Processing Magazine, 14(2) (1997) 24-41.
6. M. Hanke and P. C. Hansen, Regularization methods for large-scale problems, Surv. Math. Ind., 3 (1993) 253-315.
7. A. Tikhonov and V. Arsenin, Solution of Ill-Poised Problems, Winston, Washington, DC, 1977.
8. L. Rudin, S. Osher and E. Fatemi, Nonlinear total variation based noise removal algorithms, Physical D, 60 (1992) 259-268.
9. A. Chambolle, An algorithm for total variation minimization and applications, J. Math. Imag. Vis., 20 (2004) 89-97.
10. Y.L.Wang, J.F.Yang, W.T.Yin and Y.Zhang, A new alternating minimization algorithm for total variation image reconstruction, SIAM J. Imag. Sci., 1(3) (2008) 248-272.
11. C.R.Vogel, Computational Methods for Inverse Problems, SIAM, Philadelphia, 2002.
12. T. F. Chan, G. H. Golub and P. Mulet, A nonlinear primal-dual method for total variation-based image restoration, SIAM J. Sci. Comput., 20(6) (1999) 1964-1977.
13. J.P.Olivira, J.M.Bioucas-Dias, M.A.T.Figueiredo, Adaptive total variation image deblurring: A majorization-minimization approach, Singal Process., 89 (2009) 1683-1693.
14. A. Beck and M. Teboulle, Fast gradient-based algorithms for constrained total variation image denoising and deblurring problems, IEEE Trans. Image Process., 18(11) (2009) 2419-2434.
15. S. Becker, J. Bobin, E. J. Candes, NESTA: a fast and accurate first-order method for sparse recovery, SIAM J. Imag. Sci., 4(1) (2011) 1-39.
16. M. Bertero and P. Boccacci, Introduction to Inverse Problems in Imaging, Inst. of Physics Publ. London, UK, 1998.
17. P.C.Hansen, Discrete Inverse Problems: Insight and Algorithms, SIAM, Philadelphia, 2010.
18. D.Strong and T.Chan, Spatially and scale adaptive total variation based regularization and anisotropic diffusion in image processing, Technical report, UCLA, 1996.
19. D.Strong, J.-F.Aujol and T.Chan, Scale recognition, regularization parameter selection, and Meyer's G norm in total variation regularization, Technical report, UCLA, 2005
20. M. Bertalmio, V. Caselles, B. Rouge and A. Sole, TV based image restoration with local constraints. J. Sci. Comput., 19 (2003) 95-122.
21. A. Almansa, C. Ballester, V. Caselles and G. Haro, A TV based restoration model with local constraints, J. Sci. Comput., 34(3) (2008) 209-236.
22. Y. Q. Dong, M. Hintermuller and M. M. Rincon-Camacho, Automated regularization parameter selection in multi-Scale total variation models for image restoration, J. Math. Imag. Vis., 40(1) (2011) 82-104.
23. Z. Wang, A. C. Bovik, H. R. Sheikh, and E. P. Simoncelli, Image quality assessment: From error visibility to structural similarity, IEEE Trans. Image Process., 13(4) (2004) 600-612.